

# Measurement of the tensor $A_{yy}$ and vector $A_y$ analyzing powers of the deuteron inelastic scattering off berillium at 5.0 GeV/c and 178 mr.

L.S. Azhgirey<sup>1</sup>, S.V. Afanasiev<sup>1</sup>, A.Yu. Isupov<sup>1</sup>, V.I. Ivanov<sup>1</sup>,  
A.N. Khrenov<sup>1</sup>, V.P. Ladygin<sup>1,†</sup>, N.B. Ladygina<sup>1</sup>, A.G. Litvinenko<sup>1</sup>,  
V.V. Peresedov<sup>1</sup>, N.P. Yudin<sup>2</sup>, V.N. Zhmyrov<sup>1</sup>, L.S. Zolin<sup>1</sup>

<sup>1</sup> JINR, 141980, Dubna, Moscow Region, Russia

<sup>2</sup> Moscow State University, Moscow, Russia

**Abstract.** Tensor  $A_{yy}$  and vector  $A_y$  analyzing powers in the inelastic scattering of deuterons with the momentum of 5.0 GeV/c on beryllium at an angle of 178 mr in the vicinity of the excitation of baryonic resonances with masses up to  $\sim 1.8$  GeV/ $c^2$  have been measured. The  $A_{yy}$  data are in a good agreement with the previous data obtained at 4.5 and 5.5 GeV/c. The results of the experiment are compared with the predictions of the plane wave impulse approximation and  $\omega$ -meson exchange models.

**Keywords:** deuteron inelastic scattering, tensor analyzing power, baryonic properties.

---

<sup>†</sup>Electronic address: ladygin@sunhe.jinr.ru

# 1 Introduction

Deuteron inelastic scattering off hydrogen and nuclei at high energies has been extensively investigated at different laboratories during last years [1]-[13]. The interest to this reaction is due mainly to the possibility to study nucleon-baryon ( $NN^*$ ) interaction.

Firstly, since the deuteron is an isoscalar probe, inelastic scattering of deuterons,  $A(d, d')X$ , is selective to the isospin of the unobserved system  $X$ , which is bound to be equal to the isospin of the target  $A$ . This feature, for instance, was used to search  $\Delta\Delta$  dibaryons with an isospin  $T = 0$  in the  $d(d, d')X$  reaction [6]. Inelastic scattering of deuterons on hydrogen,  $H(d, d')X$ , in particular, is selective to the isospin 1/2 and can be used to obtain information on the formation of baryonic resonances  $N^*(1440)$ ,  $N^*(1520)$ ,  $N^*(1680)$ , and others.

On the other hand, deuteron inelastic scattering at relativistic energies involves high momentum transfers. Therefore, if the deuteron scattering take place as a result of nucleon-nucleon collisions, one may expect it to be sensitive to the structure of the deuteron and, possibly, to the manifestation of non-nucleonic degrees of freedom, namely,  $NN^*$  and  $N^*N^*$  components in the deuteron wave function [14, 15]. In this respect, inelastic scattering of deuterons on nuclei at high transferred momenta can be considered as complementary method to the elastic  $pd$ - and  $ed$ -scatterings, deuteron breakup reaction, electro- and photodisintegration of the deuteron to investigate the deuteron structure at short distances.

Third, deuteron inelastic scattering can be sensitive to the amplitudes of  $NN^* \rightarrow NN^*$  processes in the kinematical range, where the contribution of double scattering diagrams [7] is significant.

At last, since there is a large momentum transfer, one can hope to get

information on the formation of  $6q$  configuration in the deuteron.

Differential cross section measurements of deuteron inelastic scattering have been performed at Saclay at  $2.95 \text{ GeV}/c$  [1, 4] for hydrogen, at Dubna [3, 5, 7] for different targets at deuteron momenta up to  $9 \text{ GeV}/c$ , and at Fermilab [2] at higher energies for hydrogen. Calculations performed in the framework of the multiple-scattering formalism [7] have shown that the differential cross section of the  $H(d, d')X$  reaction can be satisfactorily described by hadron-hadron double scattering. The amplitudes of the elementary processes  $NN \rightarrow NN^*$  have been extracted for  $N^*(1440)$ ,  $N^*(1520)$ , and  $N^*(1680)$  resonances [7].

The availability of the polarized deuteron beams at high energies allowed to continue the investigation of the  $(d, d')X$  process, however, the polarization data on deuteron inelastic scattering are still scarce. The polarized deuterons of high energies have been used to study the tensor analyzing power  $T_{20}$  in the vicinity of the Roper resonance ( $P_{11}(1440)$ ) excitation on hydrogen and carbon targets at Dubna [8] and on hydrogen target at Saclay [9]. The measurements of  $T_{20}$  in the deuteron scattering at  $9 \text{ GeV}/c$  on hydrogen and carbon have been performed for missing masses up to  $M_X \sim 2.2 \text{ GeV}/c^2$  [10]. The experiments have shown a large negative value of  $T_{20}$  at momentum transfer of  $t \sim -0.3 (\text{GeV}/c)^2$ . Such a behaviour of the tensor analyzing power has been interpreted in the framework of the  $\omega$ -meson exchange model [16] as due to the longitudinal isoscalar form factor of the Roper resonance excitation [17]. The measurements of the tensor and vector analyzing powers  $A_{yy}$  and  $A_y$  at  $9 \text{ GeV}/c$  and  $85 \text{ mr}$  of the secondary deuterons emission angle in the vicinity of the undetected system mass of  $M_X \sim 2.2 \text{ GeV}/c^2$  have shown large values. The obtained results are in satisfactorily agreement with the plane wave impulse approximation

(PWIA) calculations [18]. It was stated that the spin-dependent part of the  $NN \rightarrow NN^*$  ( $\sim 2.2 \text{ GeV}/c^2$ ) process amplitude is significant. The measurements of  $A_{yy}$  at 4.5 GeV/c and 80 mr [12] also shown large value of the tensor analyzing power. The exclusive measurements of the polarization observables in the  $H(d, d')X$  reaction in the vicinity of the Roper resonance excitation performed recently at Saclay [13] also demonstrated large spin effects.

In this paper we report new results on the tensor and vector analyzing powers  $A_{yy}$  and  $A_y$  in deuteron inelastic scattering on beryllium target at the incident deuteron momentum of 5.0 GeV/c and  $\sim 178$  mr of the secondary emission angle. Details of the experiment are described in Sect.2. The comparison with existing data and theoretical predictions is given in Sect.3. Conclusions are drawn in Sect.4.

## 2 Experiment

The experiment has been performed using a polarized deuteron beam at Dubna Synchrotron at the Laboratory of High Energies of JINR and the SPHERE setup shown in Fig.1 and described elsewhere [11, 12]. The polarized deuterons were produced by the ion source POLARIS [19]. The sign of the beam polarization was changed cyclically and spill-by-spill, as "0", "-", "+", where "0" means the absence of the polarization, "+" and "-" correspond to the sign of  $p_{zz}$  with the quantization axis perpendicular to the plane containing the mean beam orbit in the accelerator.

The tensor polarization of the beam has been determined during the experiment by the asymmetry of protons from the deuteron breakup on berillium target,  $d + Be \rightarrow p + X$ , at zero emission angle and proton momentum of  $p_p \sim \frac{2}{3}p_d$  [20]. It was shown that deuteron breakup reaction

in such kinematic conditions has very large tensor analyzing power  $T_{20} = -0.82 \pm 0.04$ , which is independent on the atomic number of the target ( $A > 4$ ) and on the momentum of incident deuterons between 2.5 and 9.0 GeV/c [21]. The tensor polarization averaged over the whole duration of the experiment was  $p_{zz}^+ = 0.716 \pm 0.043(stat) \pm 0.035(sys)$  and  $p_{zz}^- = -0.756 \pm 0.027(stat) \pm 0.037(sys)$  in " + " and " - " beam spin states, respectively.

The stability of the vector polarization of the beam has been monitored by measuring of the asymmetry of quasi-elastic  $pp$ -scattering on thin  $CH_2$  target placed at the  $F_3$  focus of VP1 beam line. The values of the vector polarization were obtained using the results of the asymmetry measurements at the momenta 2.5 GeV/c per nucleon and  $14^\circ$  of the proton scattering angle with corresponding value of the effective analyzing power of the polarimeter  $A(CH_2)$  taken as 0.234 [22]. The vector polarization of the beam in different spin states was  $p_z^+ = 0.173 \pm 0.008(stat) \pm 0.009(sys)$  and  $p_z^- = 0.177 \pm 0.008(stat) \pm 0.009(sys)$ .

The slowly extracted beam of tensor polarized 5.0 GeV/c-deuterons with an intensity of  $\sim 5 \cdot 10^8$  particles per beam spill was incident on beryllium target a 16 cm thick positioned at  $\sim 2.4$  m downstream of the  $F_5$  focus of the VP1 beam line (see Fig.1). The intensity of the beam was monitored by an ionization chamber placed in front of the target. The beam positions and profiles at certain points of the beam line were monitored by the control system of the accelerator during each spill. The beam size at the target point was  $\sigma_x \sim 0.4$  cm and  $\sigma_y \sim 0.9$  cm in the horizontal and vertical directions, respectively.

The data were obtained for four momenta of the secondary particles between 2.7 and 3.6 GeV/c. The secondary particles emitted at  $\sim 178$  mr

from the target were transported to the focus  $F_6$  by means of 2 bending magnets ( $M_0$  and  $M_1$  were switched off) and 3 lenses doublets. The acceptance of the setup was determined via Monte Carlo simulation taking into account the parameters of the incident deuteron beam, nuclear interaction and multiple scattering in the target, in the air, windows and detectors, energy losses of the primary and secondary deuterons etc. The momentum acceptances for four cases of the magnetic elements tuning are shown in Fig.2. The momentum and polar angle acceptances were  $\Delta p/p \sim \pm 2\%$  and  $\pm 18$  mr, respectively.

The coincidences of signals from the scintillation counters  $F_{61}$ ,  $F_{62}$  and  $F_{63}$  were used as a trigger. Along with the inelastically scattered deuterons, the apparatus detected the protons originating from deuteron fragmentation. For particle identification the time-of-flight (TOF) information with a base line of  $\sim 28$  m between the start counter  $F_{61}$  and the stop counters  $F_{561}$ ,  $F_{562}$ ,  $F_{564}$  were used in the off-line analysis. The TOF resolution was better than 0.2 ns ( $1\sigma$ ). The TOF spectra obtained for all four cases of magnetic elements tuning are shown in Fig.3. At the higher momentum of the detected particles only deuterons appear in TOF spectra, however, when the momentum decreases the relative contribution of protons becomes more pronounced. In data processing useful events were selected as the ones with at least two measured time of flight values correlated. This allowed to rule out the residual background completely.

The tensor  $A_{yy}$  and vector  $A_y$  analyzing powers were calculated from the yields of deuterons  $n^+$ ,  $n^-$  and  $n^0$  for different states of the beam polarization after correction for dead time of the setup, by means of the expressions

$$A_{yy} = 2 \cdot \frac{p_z^- \cdot (n^+/n^0 - 1) - p_z^+ \cdot (n^-/n^0 - 1)}{p_z^- p_{zz}^+ - p_z^+ p_{zz}^-},$$

$$A_y = -\frac{2}{3} \cdot \frac{p_{zz}^- \cdot (n^+/n^0 - 1) - p_{zz}^+ \cdot (n^-/n^0 - 1)}{p_z^- p_{zz}^+ - p_z^+ p_{zz}^-}. \quad (1)$$

These expressions take into account different values of the polarization in different beam spin states and are simplified significantly when  $p_z^+ = p_z^-$  and  $p_{zz}^+ = -p_{zz}^-$ .

The data on the tensor  $A_{yy}$  and vector  $A_y$  analyzing powers in the deuteron inelastic scattering obtained in this experiment are given in the Table 1. The reported error bars are statistical only. The systematic errors are  $\sim 5\%$  for the both  $A_{yy}$  and  $A_y$ .

The values of the secondary deuteron momentum  $p$ , width (RMS) of the momentum acceptance  $\Delta p$ , 4-momentum  $t$ , and missing mass  $M_X$  given in the Table 1 are obtained from Monte Carlo simulation. The averaged momentum of the initial deuteron equals 4.978 GeV/c due to the energy losses in the target.

The values of the missing mass  $M_X$  given in the Table 1 were calculated under the assumption that the reaction occurs on a target with proton mass. In this case, the 4-momentum transfer  $t$  and missing mass  $M_X$  are related as follows

$$M_X^2 = t + m_p^2 + 2m_p Q, \quad (2)$$

where  $m_p$  is the proton mass and  $Q$  is the energy difference between the incident and scattered deuterons.

The dashed area on the kinematical plot given in Fig.4 demonstrates the region of 4-momentum  $t$  and missing mass  $M_X$  covered by the setup acceptance in the present experiment. The solid and dashed lines correspond to the initial deuteron momenta of 5.5 GeV/c and 4.5 GeV/c and zero emission angle [8], respectively. The hatched area shows the conditions of the experiment performed at 4.5 GeV/c and  $\sim 80$  mr [12]. One

can see that the same missing mass  $M_X$  corresponds to different  $t$  under conditions of the previous [8, 12] and present experiments. In this respect, the data obtained at 5.0 GeV/c and  $\sim 178$  mr provide new information on the  $t$  and  $M_X$  dependences of the analyzing powers  $A_{yy}$  and  $A_y$ .

### 3 Results and discussion

In Fig.5 the data on the tensor analyzing power  $A_{yy}$  in the inelastic scattering of 5.0 GeV/c deuterons on beryllium at an angle of 178 mr are shown as a function of the transferred 4-momentum  $t$  by the solid triangles. The  $A_{yy}$  has a positive value at  $|t| \sim 0.9$  (GeV/c)<sup>2</sup> and crosses a zero at larger  $|t|$ . The data on tensor analyzing power obtained at zero emission angle at 4.5 GeV/c and 5.5 GeV/c [8] on hydrogen are given by the open triangles and squares, respectively (recall that for these data  $A_{yy} = -T_{20}/\sqrt{2}$ ). The data obtained at 4.5 GeV/c and at an angle of 80 mr [12] are shown by the open circles. As it was established earlier [8, 12], there is no significant dependence of  $A_{yy}$  on the  $A$ -value of the target. The observed independence of the tensor analyzing power on the atomic number of the target indicates that the rescattering in the target and medium effects are small. Hence, nuclear targets are also appropriate to obtain information on the baryonic excitations in the deuteron inelastic scattering [8, 10, 11, 12]. One can see the general behaviour of the  $A_{yy}$  data from our experiment and previous data [8, 12] in the wide region of  $|t|$ . At small  $|t|$  ( $\leq 0.3$  (GeV/c)<sup>2</sup>)  $A_{yy}$  rises linearly up to the value of  $\sim 0.3$ , then it smoothly decreases and changes the sign at  $|t| \sim 1$  (GeV/c)<sup>2</sup>.

The  $(d, d')X$  data on  $A_{yy}$  and  $A_y$  obtained at 9 GeV/c and 85 mr at large  $|t|$  in the vicinity of the baryon excitation with the mass of  $M_X \sim 2.19$  GeV/c<sup>2</sup> [11] have been satisfactorily explained in the framework of



PWIA [12] (see Fig.6). In this model the tensor and vector analyzing powers are expressed in terms of 3 amplitudes ( $T_{00}$ ,  $T_{11}$  and  $T_{10}$ ) defined by the deuteron structure and the ratio  $r$  of the spin-dependent to spin-independent parts of the elementary process  $NN \rightarrow NN^*$

$$A_{yy}(q) = \frac{T_{00}^2 - T_{11}^2 + 4r^2 T_{10}^2}{T_{00}^2 + 2T_{11}^2 + 4r^2 T_{10}^2}, \quad (3)$$

$$A_y(q) = 2\sqrt{2}r \frac{(T_{11} + T_{00})T_{10}}{T_{00}^2 + 2T_{11}^2 + 4r^2 T_{10}^2}. \quad (4)$$

One can see that the vector analyzing power  $A_y$  is proportional to the ratio  $r$ , while the tensor analyzing power  $A_{yy}$  is sensitive to  $r$  very weakly.

The amplitudes  $T_{00}$  and  $T_{11}$  are expressed in terms of  $S$ - and  $D$ - waves of the deuteron as the following

$$\begin{aligned} T_{00} &= S_0(q/2) + \sqrt{2}S_2(q/2), \\ T_{11} &= S_0(q/2) - \frac{1}{\sqrt{2}}S_2(q/2), \end{aligned} \quad (5)$$

where  $S_0$  and  $S_2$  are the charge and quadrupole form factors of the deuteron. They are defined in the standard way

$$\begin{aligned} S_0(q/2) &= \int_0^\infty (u^2(r) + w^2(r))j_0(rq/2)dr \\ S_2(q/2) &= \int_0^\infty 2w(r) \left( u(r) - \frac{1}{2\sqrt{2}}w(r) \right) j_2(rq/2)dr, \end{aligned} \quad (6)$$

where  $u(r)$  and  $w(r)$  are  $S$ - and  $D$ - waves of the deuteron in the configuration space;  $j_0(qr/2)$  and  $j_2(qr/2)$  are the Bessel functions of the zero and second order, respectively, and  $q^2 = -t$ .

Amplitude  $T_{10}$  is also defined by the  $S$ - and  $D$ - waves of the deuteron

$$\begin{aligned} T_{10} &= \frac{i}{\sqrt{2}} \int_0^\infty \left( u^2(r) - \frac{w^2(r)}{2} \right) j_0(rq/2)dr + \\ &+ \frac{i}{2} \int_0^\infty w(r) \left( u(r) + \frac{w(r)}{\sqrt{2}} \right) j_2(rq/2)dr. \end{aligned} \quad (7)$$

The ratio of the spin-dependent to spin-independent part of the elementary amplitude of the  $NN \rightarrow NN^*$  process  $r$  is taken in the simple form [18]

$$r(q) = a \cdot q, \quad (8)$$

where  $a$  is a constant.

The curves in Fig.5 are predictions of the  $A_{yy}$  behaviour in the framework of the PWIA [18]. The solid line in Fig.5 is calculated with the deuteron wave function (DWF) for Paris potential [23], while the dashed, dotted and dash-dotted lines correspond to the DWFs for Bonn A, B and C potentials [24], respectively. One can see good agreement of the  $A_{yy}$  data from the present experiment with the PWIA calculations [18] using Paris DWF.

The deviation of the data obtained in the previous experiments [8, 12] at  $|t| \sim 0.3 \div 0.8$  (GeV/c)<sup>2</sup> from the predictions of PWIA, as well as the different behaviour of the tensor analyzing power in  $(d, d')X$  process and in  $ed$ - [25, 26] and  $pd$ - [27] elastic scattering indicates the sensitivity of  $A_{yy}$  to the baryonic resonances excitation via double-collision interactions [7], where the resonance is formed in the second  $NN$  collision or resonance formed in the first  $NN$  interaction elastically scatters on the second nucleon of the deuteron.

The sensitivity of the tensor analyzing power in the deuteron inelastic scattering off protons to the excitation of baryonic resonances has been pointed out in [16] in the framework of the  $t$ -channel  $\omega$ -meson exchange model. The cross section and the polarization observables can be calculated from known electromagnetic properties of the deuteron and baryonic resonances  $N^*$  through the vector dominance model. In this model the  $t$ -dependence of the tensor analyzing power in deuteron inelastic scatter-

ing is defined by the  $t$ -dependence of the deuteron form factors and the contribution of the Roper resonance due to its nonzero isoscalar longitudinal form factor [17]. In such an approximation, the tensor analyzing power is a universal function of  $|t|$  only, without any dependence on the initial deuteron momentum, if the finite values of the resonance widths are neglected. Since, the isoscalar longitudinal amplitudes of  $S_{11}(1535)$  and  $D_{13}(1520)$  vanish due to spin-flavor symmetry, while both isoscalar and isovector longitudinal couplings of  $S_{11}(1650)$  vanish identically, the tensor analyzing power  $A_{yy}$  in inelastic deuteron scattering with the excitation one of these resonances has the value of  $+0.25$  independent of  $t$  [12].

The  $t$  dependence of  $A_{yy}$  at  $M_X \sim 1550 \text{ MeV}/c^2$  and  $M_X \sim 1650 \text{ MeV}/c^2$  are shown in Figs 7 and 8, respectively. The full triangles are the results of the present experiment, open squares, circles and triangles are obtained earlier at 4.5 and 5.5 GeV/c [8, 12]. The solid curves are the results of the PWIA calculations [18] using Paris DWF [23]. The dashed lines are the expectations of the  $\omega$ -meson exchange model [16, 17]. One can see that the behaviour of  $A_{yy}$  at  $M_X \sim 1550 \text{ MeV}/c^2$  (Fig.7) is not in contradiction with the  $\omega$ -meson exchange model prediction [17], while at  $M_X \sim 1650 \text{ MeV}/c^2$  (Fig.8) some deviation from the constant value of  $+0.25$  is observed. However, as we mentioned above, at these missing masses it may be necessary to consider additional contributions from the  $F_{15}(1680)$  and  $P_{13}(1720)$  resonances, which also have a nonzero longitudinal isoscalar form factors and, therefore, can significantly affect the  $t$ -dependence of the tensor analyzing power. Note also that since we study the inclusive  $(d, d')X$  reaction, many resonances contribute at a fixed  $M_X$  due to their finite widths, while the theoretical predictions in Figs. 7 and 8 are obtained for separate contributions of the  $S_{11}(1535)$ ,  $D_{13}(1520)$  and  $S_{11}(1650)$  resonances. In this

respect, the exclusive (or semi-exclusive) measurements with the detection of the resonances decay products could help to distinguish between the contributions of the different baryonic resonances.

The values of the vector analyzing power  $A_y$  are small except the first point at  $M_X \sim 1500 \text{ MeV}/c^2$ . In the framework of PWIA [18] such a fact can be considered as a significant role of the spin-dependent part of the elementary amplitude of the  $NN \rightarrow NN^*$  process.

The behaviour of the vector analyzing power  $A_y$  obtained in the present experiment is plotted in Fig.9 versus  $t$ . The curves are obtained using the expression (4) with the ratio  $r$  of the spin-dependent to spin-independent parts of the  $NN \rightarrow NN^*$  process taken in the form (8) with the value of  $a = 1.0$ . The solid curve in Fig.9 is obtained with the DWF for Paris potential [23], while the dashed, dotted and dash-dotted lines correspond to the DWFs for Bonn A, B and C potentials [24], respectively. The PWIA calculations give approximately the same results at the value of  $a \sim 0.8 \div 1.2$ . It should be noted that  $a$  value might have different values for the different  $M_X$ , however, we took the fixed value for the simplicity due to lack of the data.

## 4 Conclusions

We have presented data on the tensor and vector analyzing powers  $A_{yy}$  and  $A_y$  in inelastic scattering  $(d, d')X$  of  $5.0 \text{ GeV}/c$  deuterons on beryllium at an angle of  $\sim 178 \text{ mr}$  in the vicinity of the excitations of the baryonic masses from  $1.5$  up to  $1.8 \text{ GeV}/c^2$ . This corresponds to the range of 4-momentum  $|t|$  between  $0.9$  and  $1.5 \text{ (GeV}/c)^2$ .

The data on  $A_{yy}$  are in good agreement with the data obtained in previous experiments at the momenta between  $4.5 \text{ GeV}/c$  and  $5.5 \text{ GeV}/c$  [8, 12]

when they are compared versus variable  $t$ .

It is observed also that  $A_{yy}$  data from the present experiment are in good agreement with PWIA calculations [18] using conventional DWFs [23, 24]. On the other hand, the behaviour of the  $A_{yy}$  data obtained in the vicinity of the  $S_{11}(1535)$  and  $D_{13}(1520)$  resonances is not in contradiction with the predictions of the  $\omega$ -meson exchange model [17], while at higher excited masses this model may require taking into account the additional baryonic resonances with nonzero longitudinal form factors.

The vector analyzing power  $A_y$  has a large value at  $M_X \sim 1500$  MeV/ $c^2$ , that could be interpreted as a significant role of the spin-dependent part of the elementary amplitude of the  $NN \rightarrow NN^*$  reaction.

Exclusive polarization experiments [13] with the detection of the resonances decay products could significantly advance the understanding of the mechanism of the different baryonic resonances excitation and spin properties of their interactions with nucleons.

Authors are grateful to the LHE accelerator staff and POLARIS team for providing good conditions for the experiment. They thank I.I. Migulina for the help in the preparation of this manuscript. This work was supported in part by the Russian Foundation for Fundamental Research (grant No. 03-02-16224).

## References

- [1] J. Banaigs, et al., Phys.Lett. **B45**, 535 (1973)
- [2] Y. Akimov, et al., Phys.Rev.Lett.**35**, 763 (1975)
- [3] L.S. Azhgirei, et al., Yad.Fiz.**27**, 1027 (1978) [Sov.J.Nucl.Phys.**27**, 544 (1978)]; L.S. Azhgirei, et al., Yad.Fiz.**30** 1578 (1979)

- [Sov.J.Nucl.Phys.**30**,818 (1979)]
- [4] R. Baldini Celio, et al., Nucl.Phys. **A379**, 477 (1982)
- [5] V.G. Ableev, et al., Yad.Fiz.**37** 348 (1983) [Sov.J.Nucl.Phys.**37**, 209 (1983)]
- [6] M.P. Combet, et al., Nucl.Phys. **A431**, 703 (1984)
- [7] L.S. Azhgirei, et al., Yad.Fiz.**48**, 1758 (1988) [Sov.J.Nucl.Phys.**48**, 1058 (1988)]
- [8] L.S. Azhgirey, et al., Phys.Lett. **B361**, 21 (1995)
- [9] Experiment LNS-E250 (unpublished)
- [10] L.S. Azhgirey, et al., JINR Rapid Comm. **2[88]-98**, 17 (1998)
- [11] L.S. Azhgirey, et al., Yad.Fiz.**62**, 1796 (1999) [Phys.Atom.Nucl.**62**, 1673 (1999)]
- [12] V.P.Ladygin, L.S.Azhgirey, S.V.Afanasiev et al., Eur.Phys.J. **A8**, 409 (2000); L.S.Azhgirey, V.V.Arhipov, S.V.Afanasiev, et al., Yad.Fiz.**64**, 2046 (2001) [Phys.Atom.Nucl.**64**, 1961 (2001)]
- [13] L.V.Malinina, G.D. Alkhazov, W. Augustyniak, et al., Phys.Rev. **C64**, 064001 (2001)
- [14] L. Glozman, Prog.Part.Nucl.Phys. **34**, 123 (1995)
- [15] L.S. Azhgirey and N.P. Yudin, Yad.Fiz. **63**, 2280 (2000) [Phys.Atom.Nucl.**63**, 2184 (2000)]
- [16] M.P. Rekalov and E. Tomasi-Gustafsson, Phys.Rev. **C54**, 3125 (1996)

- [17] E. Tomasi-Gustafsson, M.P. Rekaló, R. Bijker, A. Leviatan and F. Iachello, *Phys.Rev.* **C59**, 1526 (1999)
- [18] V.P. Ladygin and N.B. Ladygina, *Yad.Fiz.* **65**, 188 (2002) [*Phys.Atom.Nucl.***65**, 182 (2002)]
- [19] N.G. Anishchenko, et al., *in Proceedings of the 5-th Int. Symp. on High Energy Spin Physics, Brookhaven, 1982* (AIP Conf. Proc. N95, N.Y., 1983) p.445
- [20] L.S. Zolin, et al., *JINR Rapid Comm.* **2[88]-98**, 27 (1998)
- [21] C.F. Perdrisat, et al., *Phys. Rev.Lett.* **59**, 2840 (1987);  
V. Punjabi, et al., *Phys. Rev.* **C39**, 608 (1989);  
V.G. Ableev, et al., *Pis'ma Zh.Eksp.Teor.Fiz.* **47**, 558 (1988);  
*JINR Rapid Comm.* **4[43]-90**, 5 (1990);  
T. Aono, et al., *Phys.Rev.Lett.* **74**, 4997 (1995)
- [22] L.S. Azhgirey, et al., *PTE* **1**, 51 (1997)[*Instr. and Exp.Tech.***40**, 43 (1997)]; L.S. Azhgirey, et al., *Nucl.Instr.Meth. in Phys.Res.* **A497**, 340 (2003)
- [23] M. Lacombe, et al., *Phys.Lett.* **B101**, 139 (1981)
- [24] R. Machleidt, et al., *Phys.Reports* **149**, 1 (1987)
- [25] M. Garcon, et al., *Phys.Rev.* **C49**, 2516 (1994), and references therein
- [26] D. Abbott, et al., *Phys.Rev.Lett.* **84**, 5053 (2000)
- [27] V. Ghazikhanian, et al., *Phys.Rev.* **C43**, 1532 (1991)

Table 1. The tensor  $A_{yy}$  and vector  $A_y$  analyzing powers of the inelastic scattering of 5.0 GeV/c deuterons on beryllium at an angle of  $\sim 178$  mr.

$p \pm \Delta p,$ $GeV/c$	$t,$ $(GeV/c)^2$	$M_X,$ $GeV/c^2$	$A_{yy} \pm dA_{yy}$	$A_y \pm dA_y$
$2.747 \pm 0.060$	$-1.461$	$1.776$	$0.108 \pm 0.120$	$-0.538 \pm 0.168$
$3.042 \pm 0.067$	$-1.206$	$1.716$	$-0.128 \pm 0.106$	$0.101 \pm 0.145$
$3.340 \pm 0.070$	$-1.023$	$1.627$	$0.097 \pm 0.068$	$-0.020 \pm 0.097$
$3.638 \pm 0.077$	$-0.901$	$1.508$	$0.182 \pm 0.054$	$0.373 \pm 0.076$



## Figure captions

Fig.1. Layout of the SPHERE setup with beam line  $VP1$ .  $M_i$  and  $L_i$  designate magnets and lenses, respectively;  $IC$  is ionization chamber;  $T$  is target;  $F_{61}$ ,  $F_{62}$ ,  $F_{63}$  are trigger counters;  $F56_{1-4}$  are scintillation counters and  $HT$  is scintillation hodoscope for TOF measurements;  $H0XY$  and  $H0UV$  are beam profile hodoscopes.

Fig.2. The momentum acceptances of the setup for deuterons for different magnetic elements tuning. The panels a), b), c) and d) correspond to the secondary deuteron momenta of 2.7, 3.0, 3.3 and 3.6 GeV/c, respectively.

Fig.3. The TOF spectra obtained for different magnetic elements tuning. The panels a), b), c) and d) correspond to the secondary deuteron momenta of 2.7, 3.0, 3.3 and 3.6 GeV/c, respectively.

Fig.4. The kinematical plot of the missing mass  $M_X$  versus 4-momentum  $t$  at the initial deuteron momenta between 4.5 and 5.5 GeV/c. The solid and dashed lines correspond to the conditions (middle of the acceptance) of the experiment performed at zero angle at 5.5 GeV/c and 4.5 GeV/c, respectively [8]. The dashed area demonstrates the region of 4-momentum  $t$  and missing mass  $M_X$  covered within the acceptance of the present experiment, while the hatched area shows the conditions of the experiment performed at 4.5 GeV/c and  $\sim 80$  mr [12].

Fig.5. Tensor analyzing power  $A_{yy}$  in deuteron inelastic scattering on beryllium at 5.0 GeV/c at an angle of 178 mr and at 4.5 GeV/c at an angle of 80 mr [12] given by the full and open triangles, respectively; on hydrogen at 4.5 and 5.5 GeV/c at zero angle [8] shown by the open triangles and squares, respectively, as a function of the 4-momentum  $t$ . The solid,

dashed, dotted and dash-dotted lines are predictions in the framework of PWIA [18] using DWFs for Paris [23] and Bonn A, B and C [24] potentials, respectively.

Fig.6. Diagram of the plane wave impulse approximation for deuteron inelastic scattering with the baryonic excitation.

Fig.7. The  $A_{yy}$  data from the present experiment (full triangles) along with the data obtained with 4.5 and 5.5 GeV/c deuterons at zero angle [8] (open circles and squares, respectively) and the data at 4.5 GeV/c at an angle of 80 mr [12] plotted versus 4-momentum  $t$  for the missing mass  $M_X \sim 1550$  MeV/c<sup>2</sup>. The solid curve is the calculations in PWIA using DWFs for Paris [23]. The dashed line is the predictions within the  $\omega$ -meson exchange model [17].

Fig.8. The  $A_{yy}$  data from the present experiment (full triangles) along with the data obtained with 4.5 and 5.5 GeV/c deuterons at zero angle [8] (open circles and squares, respectively) and the data at 4.5 GeV/c at an angle of 80 mr [12] plotted versus 4-momentum  $t$  for the missing mass  $M_X \sim 1650$  MeV/c<sup>2</sup>. The solid curve is the calculations in PWIA using DWFs for Paris [23]. The dashed line is the predictions within the  $\omega$ -meson exchange model [17].

Fig.9. Vector analyzing power  $A_y$  in deuteron inelastic scattering on beryllium at 5.0 GeV/c at an angle of 178 mr as a function of the 4-momentum  $t$ . The solid, dashed, dotted and dash-dotted lines are predictions in the framework of PWIA [18] using DWFs for Paris [23] and Bonn A, B and C [24] potentials, respectively.

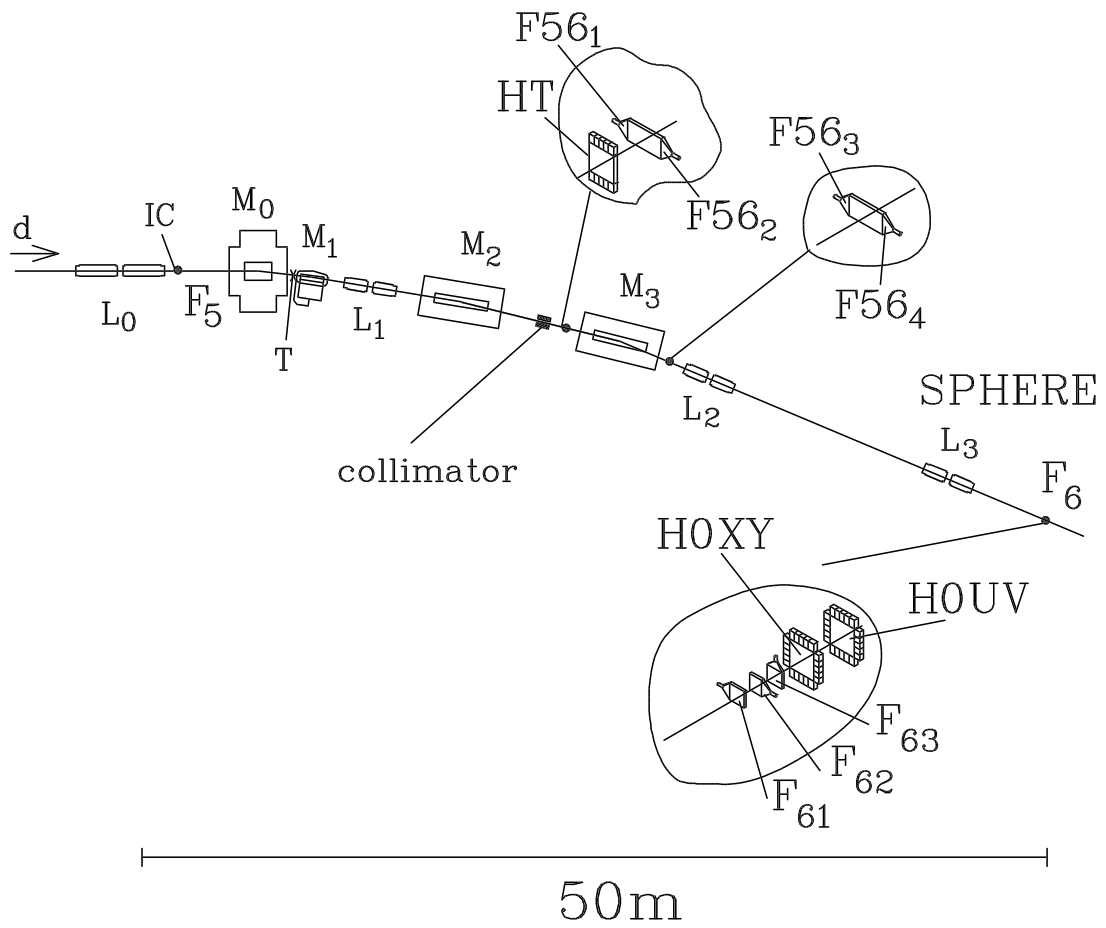


Figure 1:

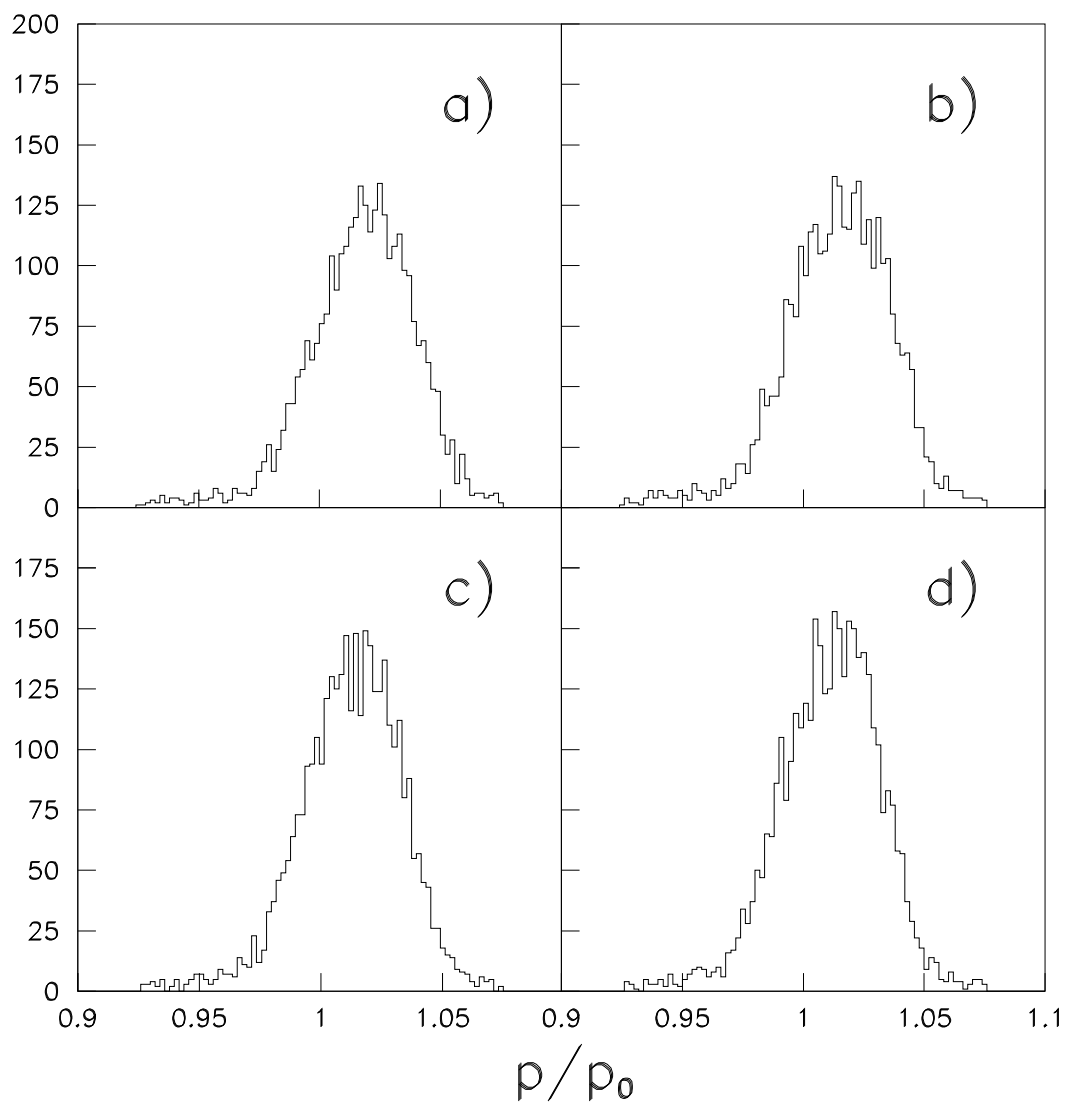


Figure 2:

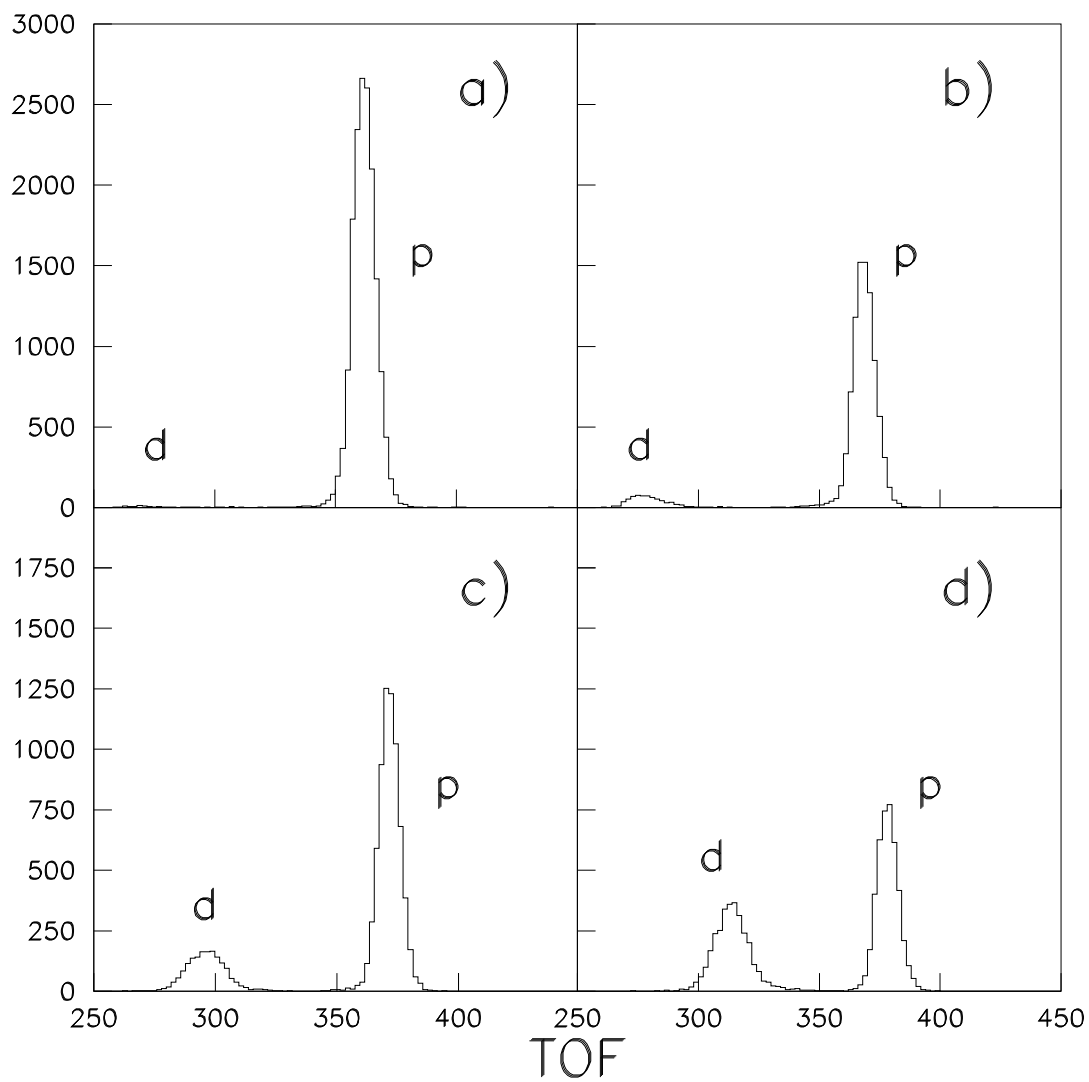


Figure 3:

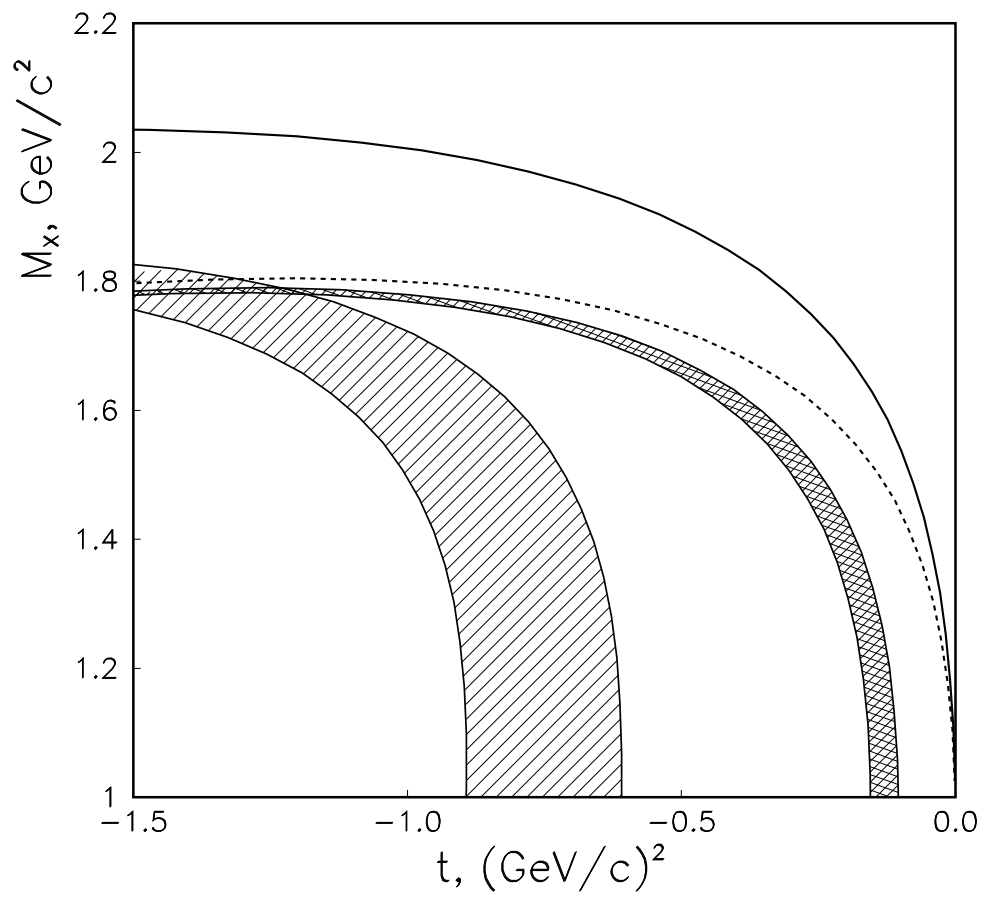


Figure 4:

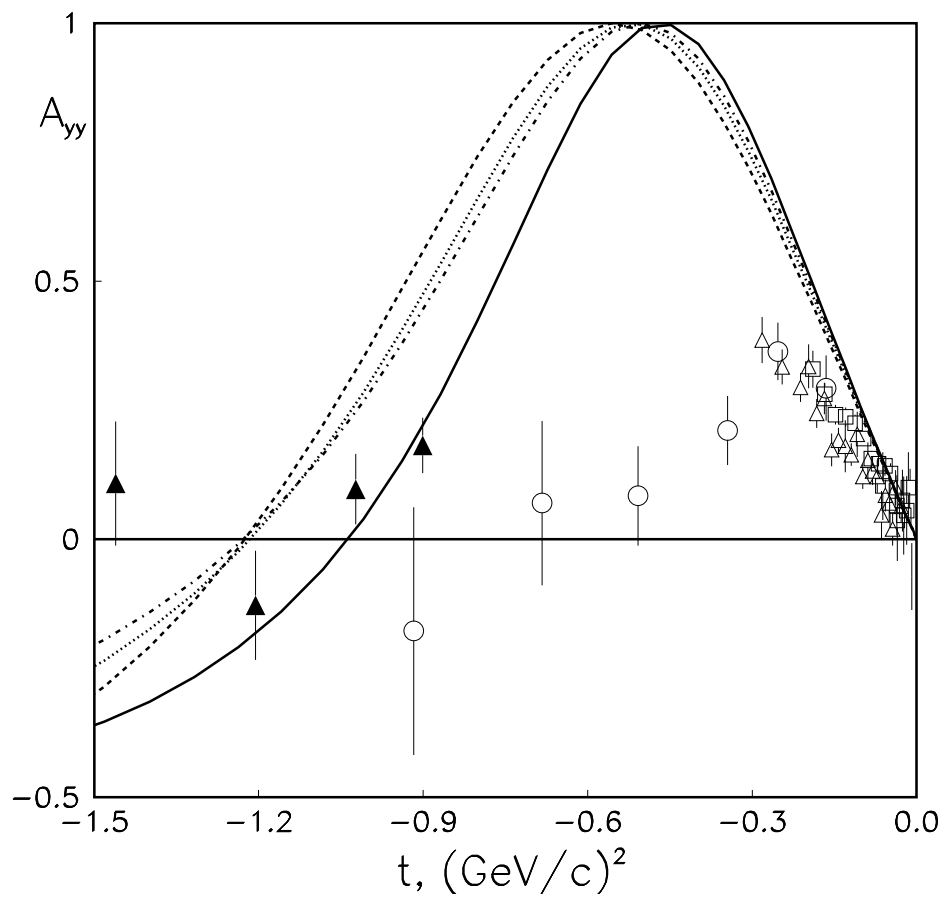


Figure 5:

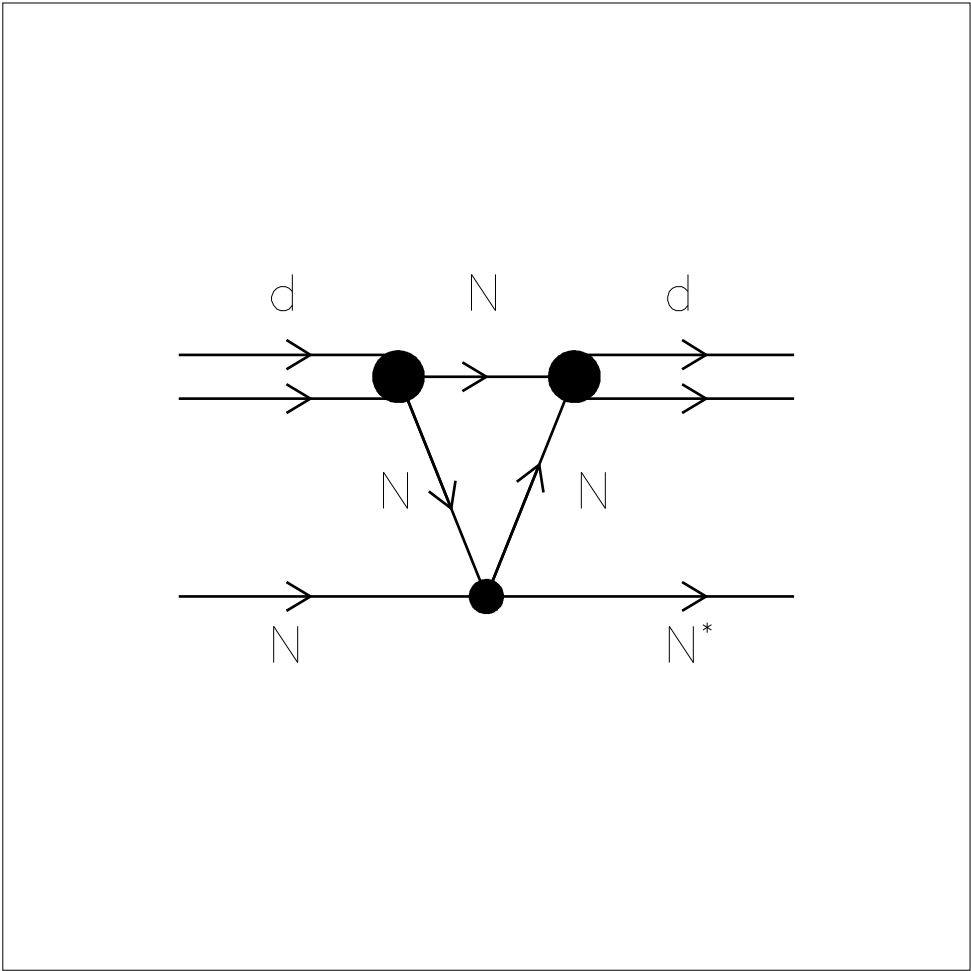


Figure 6:



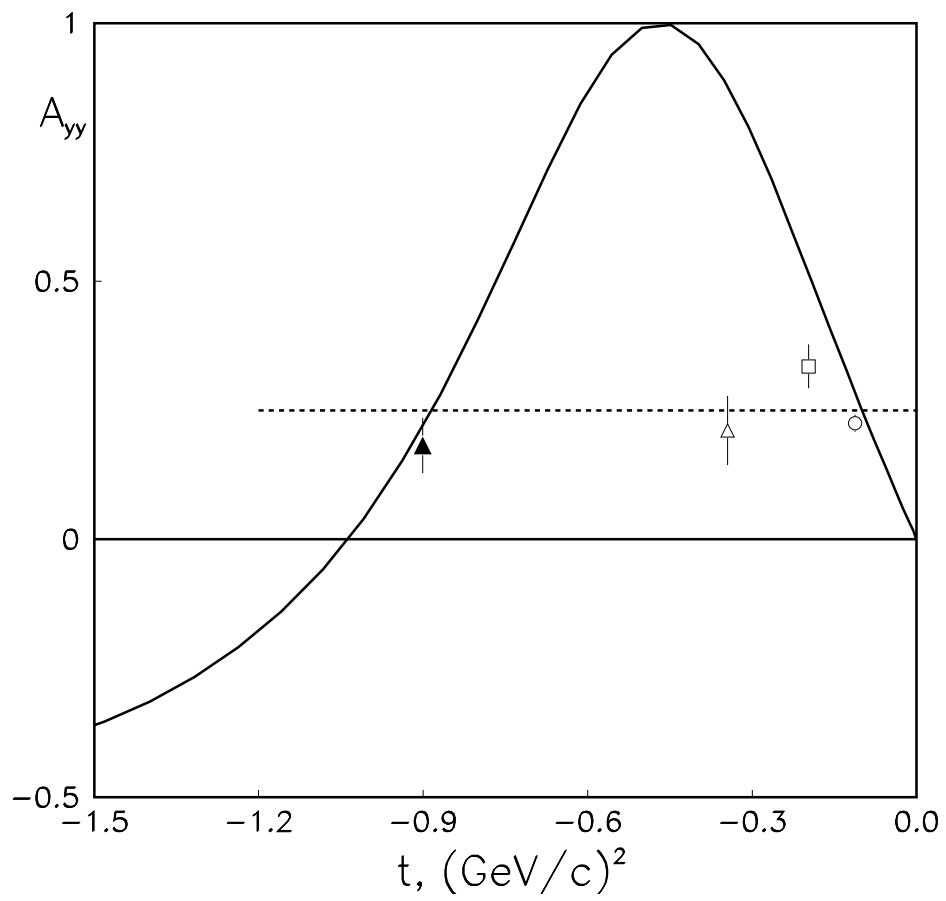


Figure 7:

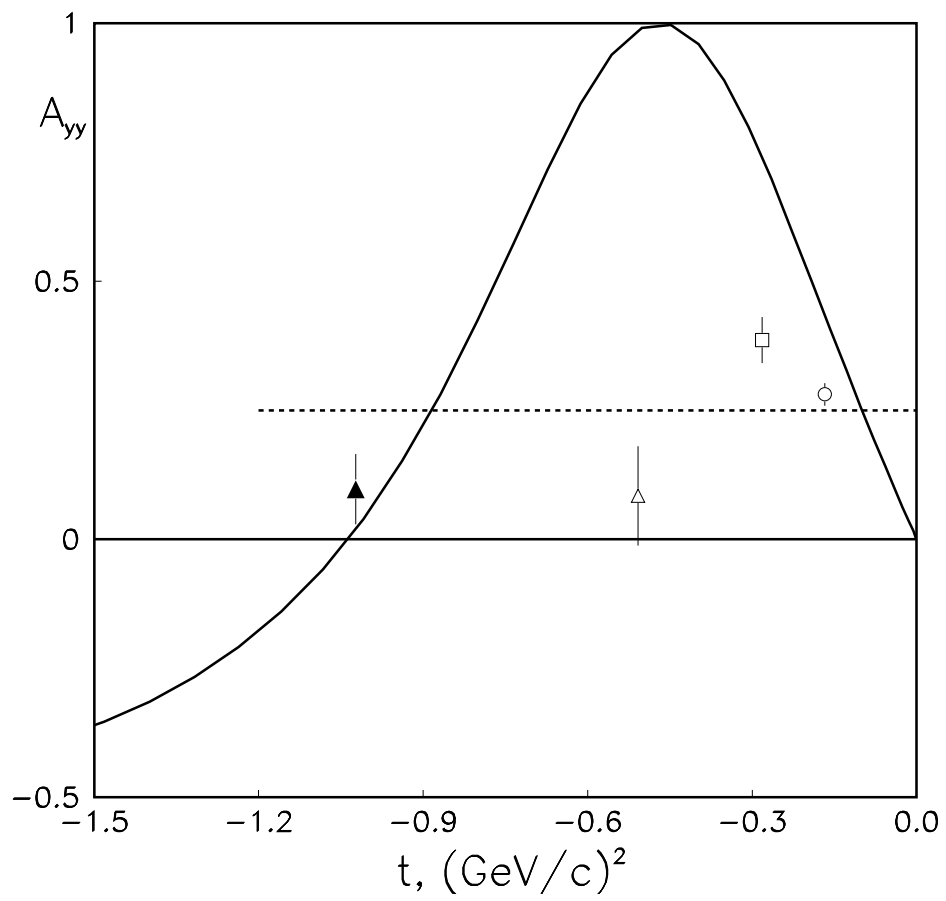


Figure 8:

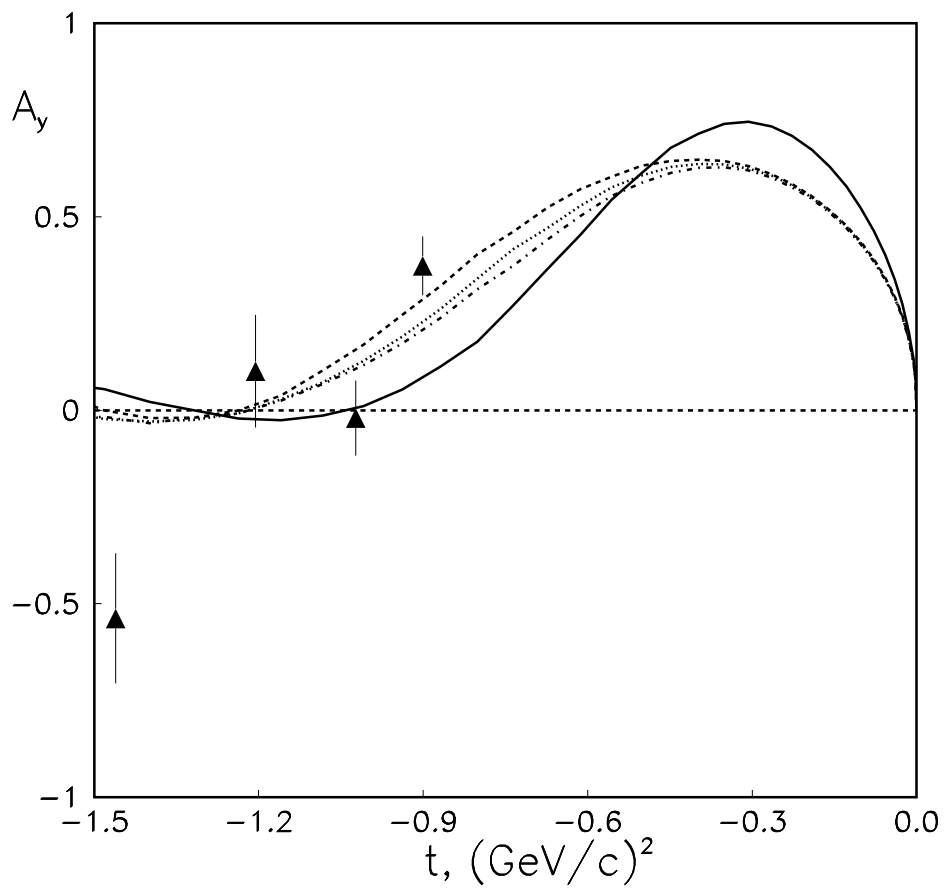


Figure 9: